

HYDROGEN PERMEABILITY AND DIFFUSIVITY IN HYDROGEN TRANSFER PIPELINES: THE EFFECT OF HYDROGEN PRESSURE

Henry Osabohien
Technical Support Department,
ADNOC Onshore,
P.O. Box 270, Abu Dhabi, United Arab Emirates.

Abstract: The design of new hydrogen delivery pipelines considers the potential for hydrogen permeability, diffusivity, and embrittlement of pipelines. This study investigates the effect of hydrogen pressure on hydrogen permeability and diffusivity in hydrogen transfer pipelines. PSL-2, API 5L X42, X52, and X60 pipes are chosen for the tests using a high-pressure hydrogen permeation tester. The microstructures of the pipe materials are analysed using optical microscopes and thereafter tested for hydrogen permeability and diffusivity up to 725 psi and at 40°C. The results indicate that the grade X52 pipe material exhibits higher diffusivity and permeability than the grades X42 and X60 pipes, primarily because of inhomogeneity in its microstructure, a result of inadequate control during the thermomechanical processing of the pipe. The results also depict an increase in hydrogen permeability and diffusivity with higher hydrogen pressure.

Keywords: Hydrogen embrittlement; hydrogen gas; hydrogen pressure; hydrogen pipeline; hydrogen permeability; hydrogen diffusivity.

I. INTRODUCTION

Hydrogen is an important energy carrier that can play a very significant role in tackling critical energy challenges. It is odourless, colourless, tasteless, non-toxic, and non-corrosive, but it can embrittle metals [1]. Hydrogen is known to be the lightest element and a clean substitute for natural gas [1]. It is the most abundant chemical substance, estimated to constitute about 75% of the universe's mass [2]. Hydrogen is highly flammable and heats up with reduced pressure. In terms of handling, it is one of the most difficult gases to keep from leaking. It burns in the air with a pale blue colour and has a virtually undetectable flame [3]. In air, hydrogen has a lower flammability limit (LFL) of 4% and an upper flammability limit (UFL) of 75% [3].

Hydrogen can be transported through pipelines the same way natural gas is today [4]. Transporting gaseous hydrogen through existing pipelines is a cost-effective alternative to delivering hydrogen in large volumes. One of the major impediments to expanding hydrogen pipelines is the high capital cost.

The design of new hydrogen transfer pipelines takes into account the potential for hydrogen permeation, diffusivity, leaks, and embrittlement. Hydrogen embrittlement is a process that occurs when metals' ductility and fracture toughness decrease due to the presence of hydrogen atoms [10]. In high-stress regions, hydrogen accumulates and may reach critical amounts, which could result in disastrous consequences [22]. The microstructure of the material and the amount of hydrogen absorbed determine the level of embrittlement. The hydrogen embrittlement process becomes significant when it results in cracking [12]. Cracking due to hydrogen embrittlement occurs when stress is applied to the embrittled object. Such stress can exist due to residual stress. Hydrogen supports subcritical cracking and increases the growth rate of fatigue cracks [11]. Crack growth resulting from hydrogen may occur very rapidly if the environmental conditions suitable for hydrogen to enter the metal are sufficiently available [21]. Failure due to crack growth may occur instantaneously or take a longer time, depending on the metal's susceptibility.

Over the years, several studies have been carried out on hydrogen embrittlement in pipelines, but little emphasis has been placed on understanding the effect of hydrogen pressure as a major contributing factor to the processes of hydrogen permeation and diffusivity. Mohtadi-Bonab and Masoumi [20] discussed extensively the different aspects of hydrogen diffusion behaviour in pipelines. Laadel, El Mansori, Kang, Marlin, and Boussant-Roux [19] highlighted the permeation barriers for hydrogen embrittlement prevention in metals, as well as other relevant studies. This work attempts to bridge the gap by employing experimental measurements to investigate the impact of

hydrogen pressure on hydrogen diffusivity and permeation in hydrogen transfer pipelines.

II. THEORETICAL AND CONCEPTUAL FRAMEWORK

The use of steel pipes for hydrogen transportation requires a systematic engineering design so that the pipeline system continues to operate under a safe threshold within its design life. The level of hydrogen embrittlement depends significantly on hydrogen pressure. Hydrogen solubility and concentration significantly influence the rate of mechanical property degradation in steel pipes [9]. The level of hydrogen diffusivity influences the rate of crack propagation, while the hydrogen absorption/surface effect determines the rate and volume of hydrogen entering the pipe [9].

Metals exhibit hydrogen embrittlement in three main categories [10]:

1) Hydrogen environmental embrittlement (HEE),

2) Internal hydrogen embrittlement (IHE),
3) Hydrogen reaction embrittlement (HRE).

Metals exposed to a high-pressure gaseous hydrogen environment experience the HEE condition [10]. IHE exists when the hydrogen source is from electrochemical processes, e.g., cathodic charging, thermal charging, corrosion, casting, electroplating, pickling, welding, etc. [10, 20]. HRE exists when metals chemically react with hydrogen, which can occur without the application of external stress [10].

Three factors contribute to accelerated hydrogen embrittlement conditions [9], viz.

- 1) Tri-axial stress state of pipeline (applied stress),
- 2) Susceptible microstructure (material type),
- 3) Diffusible hydrogen inclusion (hydrogen environment).

Fig. 1 illustrates the three factors that contribute to accelerated hydrogen embrittlement with respect to the three main categories of hydrogen embrittlement.

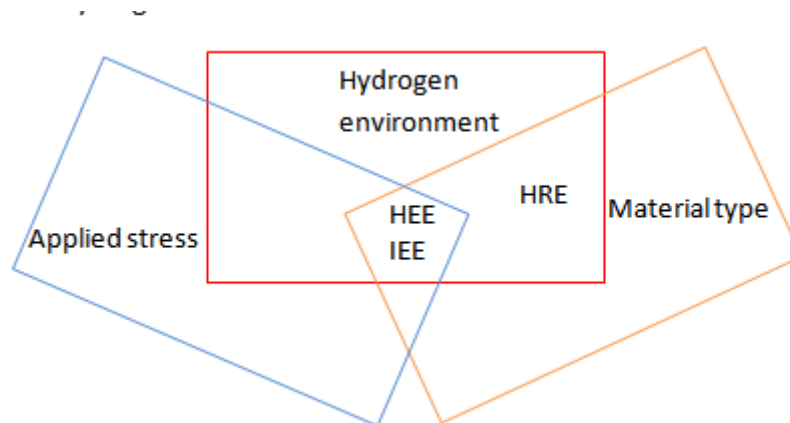


Fig. 1. HEE, IHE, and HRE type-based classification [10]

2.1 Hydrogen permeability

This is the diffusion of hydrogen ions through metal surfaces, either through substitutional or interstitial mechanisms [18].

Substitutional mechanism: This is also referred to as a vacancy mechanism. Sometimes vacancies or voids exist in the metal lattice, causing hydrogen to diffuse into such voids [18].

Interstitial mechanism: Under specific conditions, hydrogen molecules (H_2) can dissociate into ions (H^+) that are small

enough to diffuse through the natural lattice structures of metals without causing any displacement of the lattice structure [18].

Hydrogen pressure exposes the internal surface of a hydrogen transfer pipeline, allowing hydrogen to permeate through the pipe walls and into the atmosphere. The different stages of hydrogen permeation are described in Fig. 2.

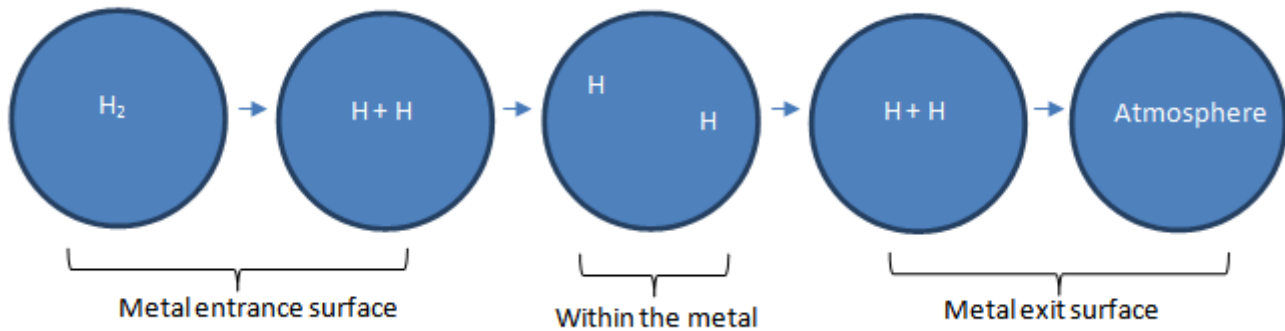


Fig. 2. Stages of hydrogen permeation

For hydrogen permeation to occur, it involves various stages [9], viz.

- 1) Metal entrance surface: Hydrogen adsorption, hydrogen dissociation, and hydrogen dissolution
- 2) Within the metal: Hydrogen diffusion and hydrogen dissociation/trapping
- 3) Metal exit surface: Hydrogen recombination and hydrogen desorption

2.2 Hydrogen diffusivity

Hydrogen diffusivity refers to the rate at which hydrogen can move through a metal. It is a major property in applications like hydrogen storage, fuel cells, and hydrogen embrittlement in metals. This process depends on several factors, such as material structure, trap density, distribution of irreversible and reversible traps, dislocation density, settling of elements in the segregated parts, temperature, and pressure [9, 20].

2.3 Reduction of hydrogen embrittlement

It is important to understand the source of the hydrogen to successfully stall the hydrogen embrittlement process. For hydrogen embrittlement in hydrogen transfer pipelines, the source of hydrogen is the transported hydrogen in direct contact with the walls of the pipe. In this case, the mitigation strategy is to limit or restrict hydrogen ingress into the pipe material. An internal surface coating or treatment can achieve this [19]. Hydrogen embrittlement can also be minimised by reducing applied and residual stresses, producing tough microstructure, reducing diffusible hydrogen by using careful cleaning procedures during welding, using low hydrogen electrodes, and other relevant control techniques such as humidity control [9]. High-strength steels are very susceptible to hydrogen embrittlement [14]. Producing alloyed steel with nickel and molybdenum compositions will reduce its susceptibility. Nickel-based alloys have a low hydrogen diffusion rate [14].

2.4 Product Specification Level (PSL)

The American Petroleum Institute (API) labels pipes for sale with different specifications. API 5L (the API standard for line pipe specifications) covers two specifications: PSL-1 and PSL-2. These specifications include both seamless and welded steel pipes, ranging from Grade A25 to X70 for PSL-1 and Grade B to X80 for PSL-2. API 5L line pipes are applicable for the transportation and distribution of water, oil, and gas [7]. For different environments, there are various requirements for API 5L line pipes. Ordinary environments use PSL-1 pipes, while severe environments or working conditions use PSL-2 pipes. Manufacturers produce PSL-2 pipes to meet the additional requirements for high temperatures, corrosive environments, gas permeation (e.g., hydrogen permeation), and other challenging conditions [7]. PSL-2 pipes possess some distinct properties that are absent in PSL-1 pipes. These properties encompass minimum notch toughness and maximums for carbon equivalent. These and other features make PSL-2 pipe materials more desirable for hydrogen transfer pipelines [17].

III. MATERIAL AND METHODS

Research was conducted to understand the impact of hydrogen pressure on hydrogen permeability and diffusivity. PSL 2, API 5L X42, X52, and X60 seamless carbon steel pipes were carefully selected for the tests due to their unique properties and widespread use in gas transmission and distribution. A high-pressure hydrogen permeation tester was used to carry out the test. The test procedure followed the guidelines provided in the framework of ASTM 1459-06 (R2012) [13]. Table 1 and Table 2 provide details of the chemical composition and tensile strength of the pipe materials used in the test.

3.1 Alloying elements of the sample carbon steel pipes

Carbon, phosphorus, silicon, sulphur, and manganese are the primary impurity elements found in carbon steel and pig iron, commonly called the “five elements.” Given their



significant influence on steel's performance, a general analysis necessitates their identification [24].

Chromium can greatly increase hardness, strength, and resistance to wear in structural steels, but it can also decrease toughness and plasticity. Chromium is an important alloying element for stainless steel and heat-resistant steel because it can increase steel's oxidation and corrosion resistance [24].

Nickel can make steel stronger while maintaining its hardness and ductility. Nickel resists rust and heat well at elevated temperatures, and it has strong corrosion resistance against acids and bases. However, because nickel is a rare resource, different alloying elements should be used instead of nickel-chromium steel [24].

Molybdenum can smooth out the steel's grain, increase heat resistance and hardenability, and preserve enough strength and resistance to creep at high temperatures. Molybdenum enhances the mechanical qualities of structural steel [24].

In steel, titanium deoxidizes quite effectively. It reduces cold brittleness, ageing sensitivity, refines grain force, and makes the internal structure of steel more solid. Improve the efficiency of welding. Adding the proper titanium to nickel

9 and chromium 18 austenitic stainless steel prevents intergranular corrosion [24].

Vanadium is a great steel deoxidizer. Adding 0.5% vanadium to steel increases its strength and toughness and refines its grain structure. Carbides made from vanadium and carbon enhance hydrogen corrosion resistance at high pressures and temperatures [24]. Copper can enhance strength and toughness, particularly against air corrosion. Adding tungsten to tool steel greatly increases its heat strength and red hardness for forging dies and cutting instruments. Niobium can improve steel's strength, lower its sensitivity to extreme heat, and moderate its brittleness; nevertheless, it also lessens the material's toughness and plasticity. Aluminium frequently deoxidizes steel. A tiny quantity of aluminium is added to enhance the steel's impact toughness and refine the grains. Mixing aluminium, chromium, and silicon greatly enhances steel's ability to withstand high temperatures and corrosion. Aluminium's impact on steel's workability, weldability, and machinability is a drawback. A trace amount of boron can enhance steel's strength, compactness, and hot-rolling qualities. Nitrogen can also enhance steel's weldability, strength, and hardness at low temperatures, as well as its ageing sensitivity [24].

Table 1. Chemical composition by percentage weight for seamless API 5L PSL 2 pipes (thickness ≤ 0.984) [16, 25]

Grade	Mass fraction,% according to product and heat analysis									Carbon equiv. a	
	C	Si	Mn	P	S	V	Nb	Ti	Oth	CE IIW max	CE Pcm max
	max b	max	Max b	max	max	max	max	max	er		
X42	0.24	0.4	1.2	0.025	0.015	0.06	0.05	0.04	e,l	0.043	0.25
X52	0.24	0.45	1.4	0.025	0.015	0.10	0.05	0.04	d,e,l	0.043	0.25
X60	0.24f	0.45f	1.40f	0.025	0.015	0.10f	0.05f	0.04f	g,h,l	As agreed	As agreed

where

a) CE limits will be as specified. $SMLS \tau > 0.787$ ". The CEIIW limits applied if $C > 0.12\%$ and the CEPcm limits apply if $C \leq 0.12\%$,

b) Increases of 0.05% above the specified maximum for Mn are allowed for every reduction of 0.01% below the maximum for C. The maximum increases are 1.65% for grades $\geq L245$ or B, but $\leq L360$ or X52; 1.75% for grades $> L360$ or X52, but $< L485$ or X70; 2.00% for grades $\geq L485$ or X70, but $\leq L555$ or X80; and 2.20% for grades $> L555$ or X80,

d) $Nb = V = Ti \leq 0.15\%$,

e) If not specified differently, $Ni \leq 0.30\%$; $Mo \leq 0.15\%$; $Cu \leq 0.50\%$; and $Cr \leq 0.30\%$,

f) If not specified differently,

g) If not specified differently, $V + Nb + Ti \leq 0.15\%$,

h) If not specified differently, $Ni \leq 0.50\%$ $Cu \leq 0.50\%$ $MO \leq 0.50\%$, and $Cr \leq 0.50\%$,

i) Unless otherwise agreed, $Cu \leq 0.50\%$ $Ni \leq 1.00\%$ $Cr \leq 0.50\%$ and $MO \leq 0.50\%$,

l) The following applies to all PSL 2 pipe grades, except those that have footnotes j indicated. Remaining B $\leq 0.001\%$ and no purposeful addition of B is allowed unless otherwise agreed.

Table 2. Tensile strength – Body of pipe (PSL 2, seamless and welded pipes) [16, 25]

Grade	Seamless pipes				Welded pipes		
	Yield strength a (psi)	Tensile strength a		Ratio a,c	Elongation Af%	Tensile strength d (psi)	
		Min	Max				Min
X42	42,200	71,800	60,200	95,200	0.93	f	60,200
X52	52,200	76,900	66,700	110,200	0.93	f	66,700
X60	60,200	81,900	75,400	110,200	0.93	f	75,400

a) Please refer to the complete API5L specification for intermediate grade.

c) Pipes with $D > 12.750$ in size are subject to this rule.

d) The established value for the pipe body with foot must coincide with the required minimum tensile strength for the weld seam on intermediate grades.

f) The following formula must be used to obtain the required minimum elongation, Af, which must be given in percentage and rounded to the nearest percent:

$$Af = C \frac{A_{xc}^{0.2}}{U^{0.9}}$$

where C is 625,000 when calculating in USC units and 1,940 when calculating in SI units.

The cross-sectional area of the appropriate tensile test piece, A_{xc} , is given as follows in square millimeters (square inches):

U is expressed in megapascals (pounds per square inch) and stands for the specified minimum tensile strength.

3.2 High-pressure hydrogen permeation tester

The high-pressure hydrogen permeation tester was designed to determine the impact of temperature, pressure, pipe surface condition, and pipe microstructure on permeability. It is an apparatus for testing the hydrogen permeation of a test piece by delivering high-pressure hydrogen to one side while analysing the hydrogen emitted from the other side through the test piece, as shown in Fig. 4. The tests were carried out up to a pressure of 725 psi and a temperature of 40°C.

The gas supply means, as shown in Fig. 3 provides high-pressure hydrogen to the primary side of the test piece. The analyser examines the hydrogen emitted from the secondary side of the test piece. The pipe connecting the gas supply means to the surface of the test piece is referred to as the primary pipe. The secondary pipe connects the other surface of the test piece to the analyser. The secondary pressure gauge measures the hydrogen pressure in the secondary pipe. The primary shut-off valve isolates the primary pipe when required. The primary release valve relates the conditions of the interior and exterior of the primary pipe when open. This valve is located downstream of the primary shut-off valve. The secondary discharge valve relates the conditions of the interior and exterior of the secondary pipe.

The passive discharge means is located in the secondary pipe. When the pressure detected by the secondary pressure gauge reaches a predefined value or higher, the primary release valve and secondary release valve open while the primary cutoff valve and the secondary cutoff valve are closed.

The test component is held so that it remains airtight on both sides, one of which is exposed to a high-pressure hydrogen environment and the other to a reduced-pressure environment. Utilising a metal gasket, O-ring, or similar seal is best. The permeation chamber is built to resist deformation when exposed to high-pressure gases. The test piece is kept in place by a holding portion with strength that can endure these conditions and extreme airtightness because the test piece is exposed to a reduced-pressure environment and high-pressure hydrogen. The test piece holder is airtight to prevent leakage of the high-pressure hydrogen inside of it. Several items can be utilized as the test piece holding portion, including items made using different known procedures. For example, the test piece holder is made of austenitic stainless steel, which has low gas emissions during temperature rise, high airtightness, high strength, good workability, low cost, etc. It is best to process the stainless steel used for ultra-high vacuum.

The side of the test piece that is attached to the surface (henceforth referred to as the "primary side") through which hydrogen enters is equipped with a high-pressure hydrogen supply mechanism. The high-pressure hydrogen supply method can be any method capable of supplying hydrogen at the required test pressure [27]. A device that uses a compressor to extract hydrogen gas from a hydrogen cylinder at the required pressure is one such application. To identify and measure the tiny quantity of hydrogen gas that has permeated through the test piece on the opposite side of the test piece, otherwise referred to as the secondary side, an analyser is installed. In the case of this experiment, a mass spectrometer was used as the analyser. A time-of-flight mass spectrometer (TOF-MS), a quadrupole mass spectrometer (QMS), a magnetic field deflection mass spectrometer, or anything similar can be employed when a mass spectrometer is used as the analyser [27]. In particular, it is better to use a device that can continually measure hydrogen at a set time interval, like every 10 seconds.

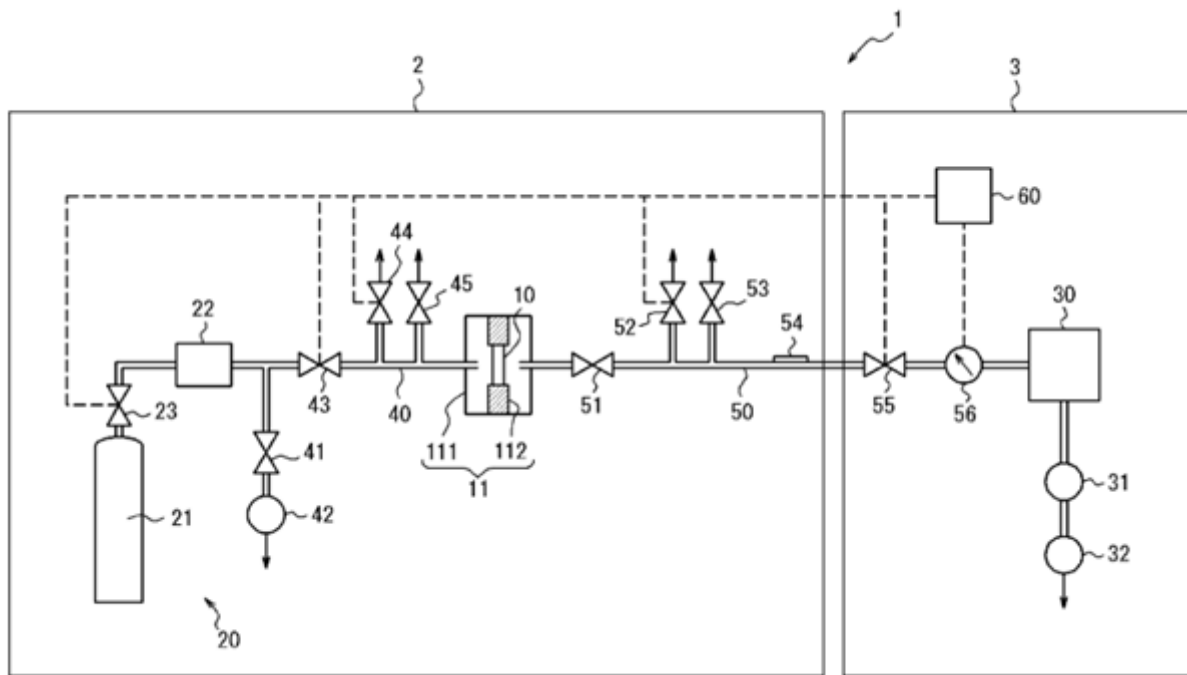


Fig. 3. High-pressure hydrogen permeation tester [27]

Description of symbols

- 1 High-pressure hydrogen permeation tester
- 2 Explosion-proof compartment
- 3 Non-explosion-proof compartment
- 10 Test piece
- 11 Holding part
- 111 Airtight chamber
- 112 Test piece holding jig
- 20 Gas supply means
- 21 Hydrogen cylinder
- 22 Compressor
- 23 Valve shutter
- 30 Quadrupole mass analyser
- 31 Turbo molecular pump
- 32 Rotary pump

- 40 Primary piping
- 41 Air drive valve
- 42 Rotary pump
- 43 Primary shutoff valve
- 44 Primary discharge valve
- 45 Safety valve
- 50 Secondary pipe
- 51 Secondary upstream shutoff valve
- 52 Secondary discharge valve
- 53 Passive discharge means
- 54 Passive discharge means
- 55 Secondary shutoff valve
- 56 Secondary pressure gauge
- 60 Control device

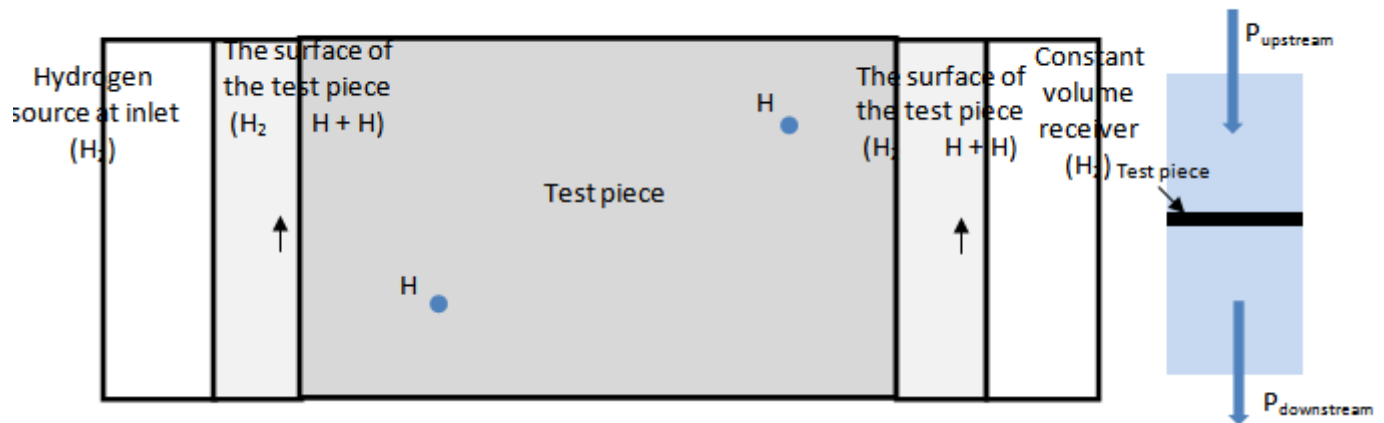


Fig. 4. High-pressure hydrogen permeation test mechanism

3.3 Microstructure analysis of the pipe materials

Investigations using metallography were conducted on the test pieces. The test pieces were cut, polished, and then etched using a cotton tip dipped in 3% nital etchant after being polished with emery paper grits of 100, 120, 320, 400, 600, 800, and 1000. The samples were then diamond polished to a 6 μ finish. The polishers were made of rotating discs coated in soft fabric, soaked in greasy lubricant and diamond particles. A 6 μ-grade particle of diamond was used to remove grinding scratches. The samples were carefully cleaned with soapy water before microstructure analysis and then dried with a fan and alcohol. The test pieces were analysed using scanning electrode microscopy (SEM). This technique generates a high-resolution image of an object by scanning its surface to make detailed, enlarged images of it [30]. It uses a concentrated electron beam to do this [30]. The generated photos provide details about the physical characteristics and composition of the object.

3.4 Data Analysis

3.4.1 Hydrogen Diffusivity

From the asymptotic slope method, effective diffusivity is determined from pressure accumulated against the time curve.

$$D_{\text{eff}} = \frac{x^2}{6t_{\text{lag}}} \quad (1)$$

D_{eff} = Effective diffusivity
 t_{lag} = Time lag
 x = Wall thickness of test piece

3.4.2 Hydrogen Permeability

Fick's first law explains hydrogen permeability [8]. It is described in Equation 2.

$$J = -D \frac{dc}{dx} \quad (2)$$

J = Hydrogen flux diffusing through the metallic membrane (test piece)

D = Hydrogen diffusion coefficient

$\frac{dc}{dx}$ = Hydrogen concentration gradient in the direction of permeation

Equation 2 can be modified to equation 3 under the condition that the coefficient of diffusion is not dependent on the concentration of hydrogen and that the hydrogen permeation attains a steady state.

$$J = D \frac{\Delta c}{x} \quad (3)$$

Δc = Hydrogen concentration difference between the inlet (feed) and the receiver side

x = Thickness of test piece

Sievert's law describes in Equation 4 the relationship between hydrogen concentration (c) and the pressure of hydrogen gas (P).

$$c = K P^{0.5} \quad (4)$$

K = Hydrogen solubility constant

The exponent 0.5 indicates the division of one hydrogen molecule into two atoms of hydrogen.

Equation 5 is derived from substituting equation 4 into equation 3.

$$J = D \cdot K \frac{\Delta P^{0.5}}{x} = \emptyset \frac{\Delta P^{0.5}}{x} \quad (5)$$

$\Delta P^{0.5}$ = Square root of the hydrogen pressure difference between the inlet (feed) and the receiver side

\emptyset = Coefficient of hydrogen permeation

IV. RESULTS AND DISCUSSION

4.1 Microstructure study of the test pieces

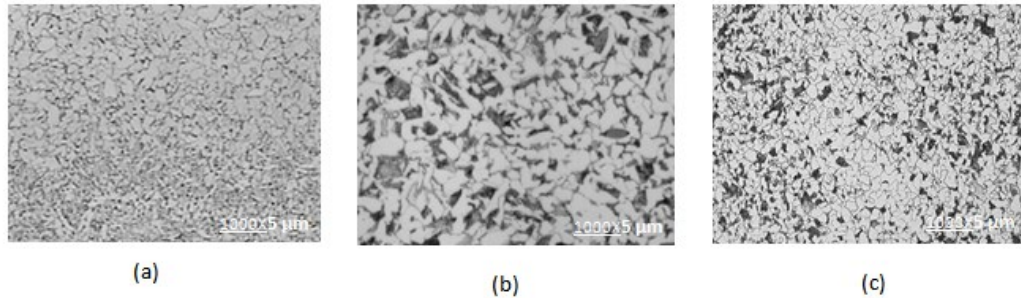


Fig. 5. Photomicrographs of test pieces, (a) API X42, (b) API 5L X52, (c) API 5L X60

As shown in Fig. 5 (a), API 5L X52 has a more heterogeneous microstructure, resulting most probably from insufficient control during the thermomechanical processing of the steel pipe. Most steel pipelines are produced by thermomechanical methods that demand several heating processes [32].

Fig. 5 displays the typical photomicrographs of the test pieces. Pearlite makes up the black portions of these structures, whereas ferrite forms the lighter portions. In general, low-carbon steels have a ferrite-pearlite structure with minimal pearlite [28, 29]. Pearlite is hard and brittle, whereas ferrite is ductile and soft [31]. The bulk strength and proportion of pearlite rise as the total carbon content increases [31]. According to earlier literature by Jian and Xiukui [33], ferrite-cementite interfaces serve as hydrogen's primary trapping sites. Reports indicate that the hydrogen trap binding energy for the ferrite-cementite interfaces is either 10.85 kJ/mol or 18.4 kJ/mol [33]. The area of the ferrite-cementite interfaces, or the amount of pearlite, increased in low-carbon steels as the carbon content increased. In other words, the rise in hydrogen trapping density is linked to the decrease in hydrogen diffusivity.

Hydrogen traps are a variety of crystal imperfections in metals that can bind with hydrogen. This binding, which prolongs the interaction between metal and hydrogen, impacts the metal's hydrogen permeability and thus its susceptibility to hydrogen embrittlement [38]. It is significant to note that voids can arise as a result of hydrogen atoms trapped in vacancies, which subsequently lead to the formation of molecular hydrogen. Due to different binding energies, trapping sites exhibit different permeation effects. Plastic deformation decreases diffusivity and increases trapping sites [5]. At room temperature, all structural metals have the potential to become embrittled by hydrogen, and the degree of sensitivity varies depending on the alloy's strength, microstructure, and other characteristics, as well as mechanical and environmental factors [34]. As a result, it is difficult to classify materials as "immune" or "susceptible" to hydrogen embrittlement. One of the most significant trends for structural metals is that the tendency for hydrogen embrittlement increases as the material's strength increases [34].

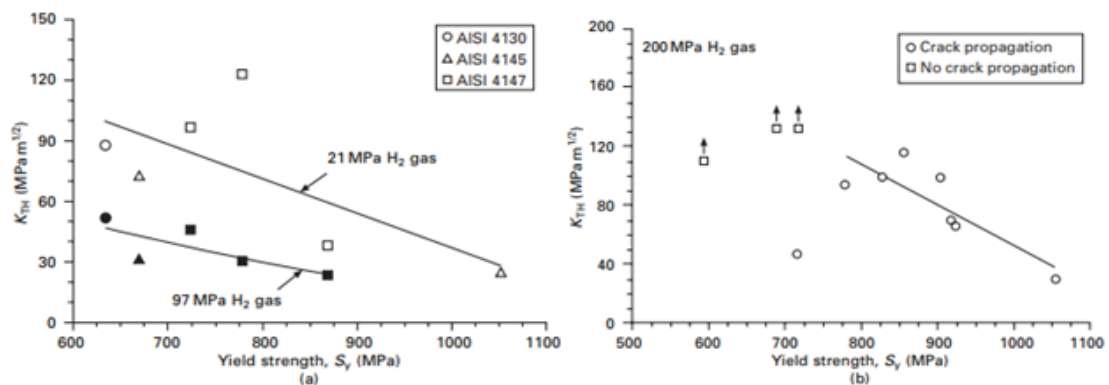


Fig. 6. Effect of yield strength on stress intensity threshold for the propagation of cracks in hydrogen gas [34]: (a) Low-alloy steel, (b) Austenitic steel.

Fig. 6 provides examples of data for low-alloy ferritic steels and austenitic steels that demonstrate how material yield strength affects the propagation of cracks in hydrogen gas. Both plots display the threshold stress intensity factor (K_{TH}), a fracture mechanics parameter that describes a material's susceptibility to subcritical crack propagation, as a metric for hydrogen embrittlement. As yield strength rises,

Fig. 6 illustrates that hydrogen embrittlement becomes more severe. When choosing materials for structures that will be exposed to hydrogen gas, they should be judged on their maximum yield strength as well as their minimum yield strength. This is because the strength of the material can have a big effect on how easily it breaks in hydrogen gas.

4.2 Hydrogen Diffusivity and Permeability

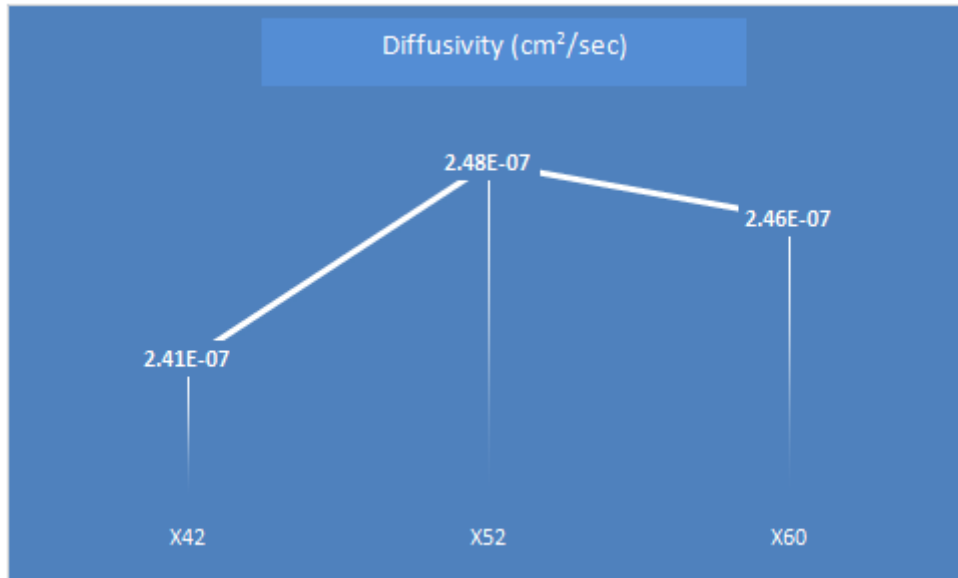


Fig. 7. Diffusivity of X42, X52 and X60 pipe materials at 500 psi

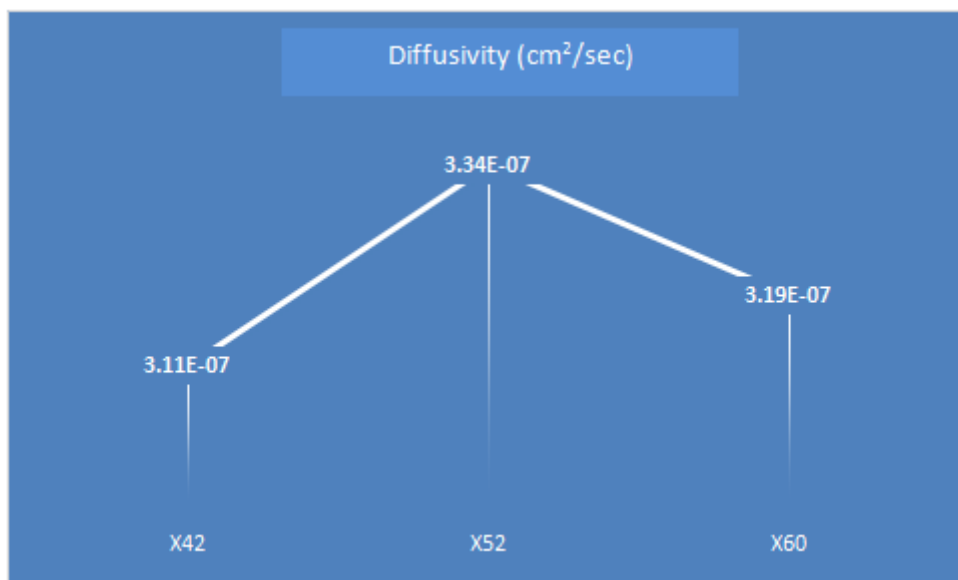


Fig. 8. Diffusivity of X42, X52 and X60 pipe materials at 725 psi

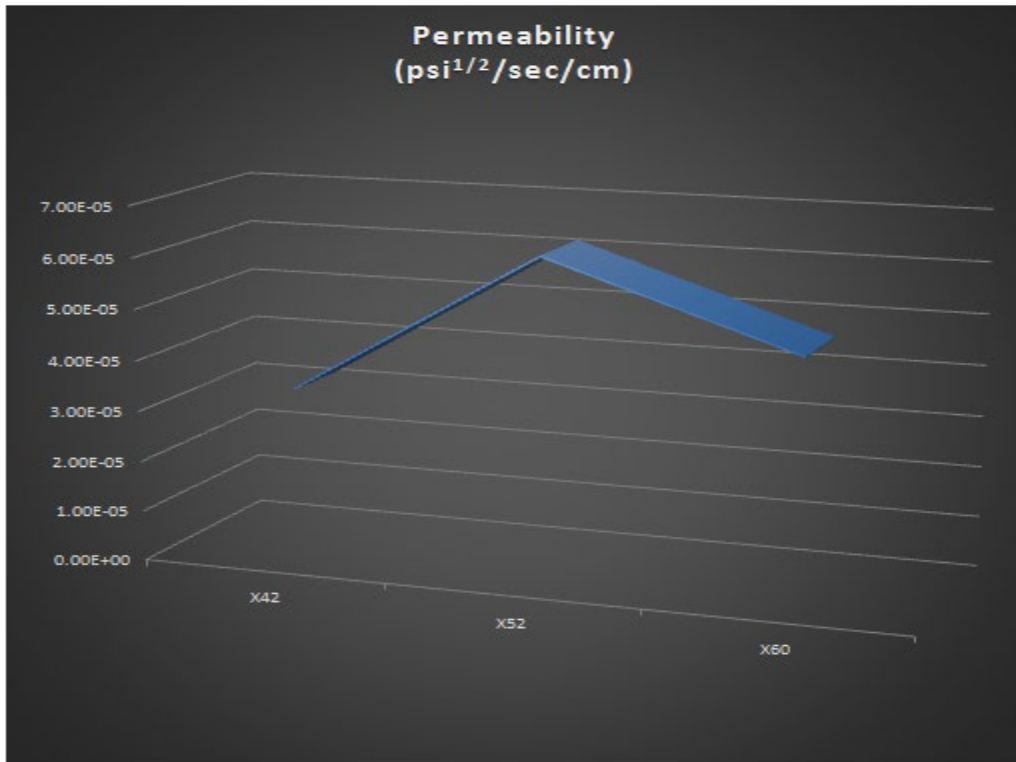


Fig. 9. Permeability of X42, X52 and X60 pipe materials at 500 psi

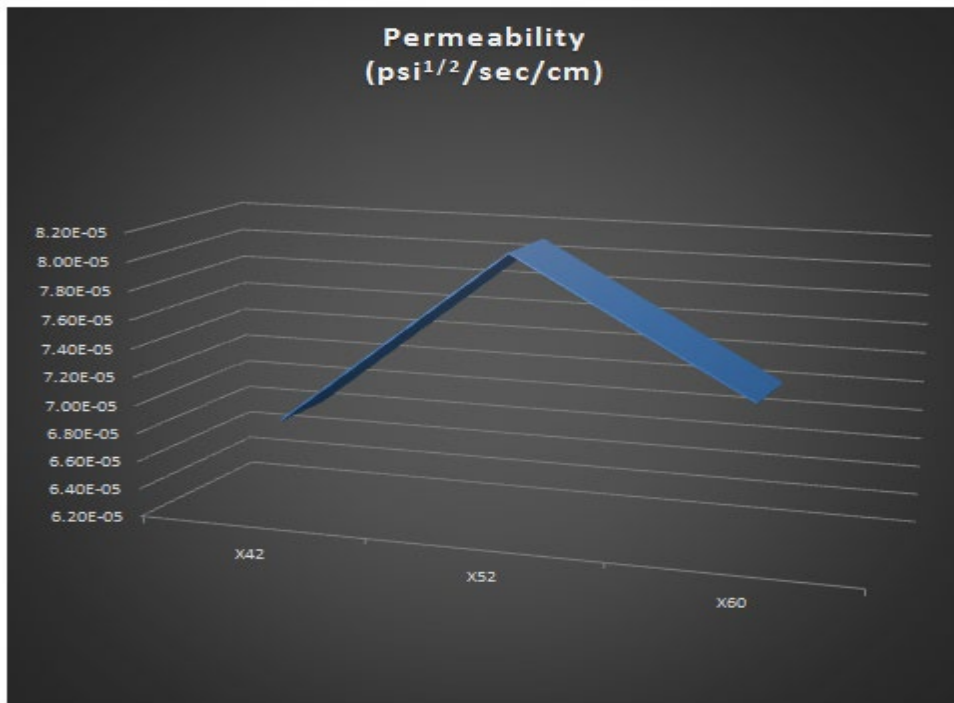


Fig. 10. Permeability of X42, X52 and X60 pipe materials at 725 psi



From the results as shown in Fig. 7, Fig. 8, Fig. 9, and Fig. 10, X52 pipes show higher diffusivity and permeability compared to X42 and X60 pipes. This corroborates earlier results from diffusivity and permeability tests applying the electrochemical technique developed by Devanathan and Stachurski [15]. It also supports the statement made by Mohtadi-Bonab and Masoumi [20] that the heterogeneity of the steel's microstructure enhances non-uniform hydrogen diffusion.

In different environments, hydrogen diffuses because of the concentration gradient. During this process, hydrogen atoms move from high-concentration areas to low-concentration areas. An awareness of the concentration gradient is required for the investigation of hydrogen diffusion dynamics. A variety of factors influence the hydrogen flow through the pipe materials. The permeation process first exhibits a stationary permeation characteristic; however, as time passes in the second stage, a progressive increase in current begins. This current increase occurs in a variety of ways. Microstructural properties such as grain size and carbide form, among other things, are likely the reasons for the changing current flow. At low temperatures, the hydrogen diffusion coefficient in the steel matrix is often relatively minimal [32]. Consequently, the steel matrix holds the majority of hydrogen in various locations known as traps, rather than in the interstices between unit cells [32]. These traps are associated with microstructural characteristics such as interfaces, microvoids, vacancies, dislocations, and impurity atoms, among other lattice flaws. Heat treatment of the steel pipe modifies the structural configuration of the carbides (Fe_3C), which take on various shapes for each one. Concerning the hydrogen solubility and diffusion constant in the steel pipe, these various forms significantly alter the permeability characteristics. The typical pearlite, which is a lamellar mixture of ferrite and cementite (carbide), is a weak hydrogen trap because of its continuous interphase, which facilitates hydrogen diffusion by acting as a free path. Sulphur and manganese inclusions are believed to be potent, irreversible hydrogen-trapping sites. These sites effectively reduce the flow of hydrogen through the material [32]. According to Souza et al. [32], several authors think that a wide range of factors can affect

how hydrogen diffuses into the microstructure. The hydrogen trapping mechanism prevents the consideration of hydrogen permeation inside the metal as a constant during the Devanathan cell test. Therefore, it is only possible to evaluate an apparent diffusion coefficient. Additionally, voids, interfaces with nonmetallic inclusions, precipitated particles, microstructure, inclusions, dislocations, grain boundaries, morphologies, and vacancies can all function as traps and influence the flow of hydrogen through a material. Fick's equations govern the diffusion mechanism, connecting hydrogen reactivity with bulk traps to hydrogen diffusibility.

Taking a look at the test pieces from the experiment, it is likely that the rate of crack propagation is higher in X52 pipes due to the strong influence of hydrogen diffusivity [9]. Hydrogen causes fatigue crack propagation, creates new material failure modes, and decreases conventional fracture resistance metrics such as ductility, tensile strength, and fracture toughness [34].

4.4 Effect of hydrogen pressure

Fig. 7, Fig. 8, Fig. 9, and Fig. 10 indicate that diffusivity and permeability increased with higher hydrogen pressure. The test pieces had higher rates of diffusivity and permeability at 725 psi than at 500 psi.

Higher hydrogen gas pressure causes structural metals to become more vulnerable to hydrogen embrittlement. Sievert's law represents the thermodynamic equilibrium between hydrogen gas and dissolved atomic hydrogen, as $C = S\text{P}^{1/2}$. This relationship indicates that the amount of atomic hydrogen dissolved in the material increases with pressure, which subsequently causes embrittlement to worsen. Fig. 11 provides an example of how gas pressure generally affects hydrogen embrittlement. The observations of fracture toughness in hydrogen gas (K_{IH}) and threshold stress-intensity factor for crack propagation in hydrogen gas (K_{TH}) are displayed against hydrogen gas pressure in this figure. The K_{IH} results pertain to carbon steel, whereas the K_{TH} data pertain to low-alloy steel. Fig. 11 illustrates how K_{TH} and K_{IH} both decrease with increasing gas pressure, suggesting greater chances of hydrogen embrittlement at higher pressure.

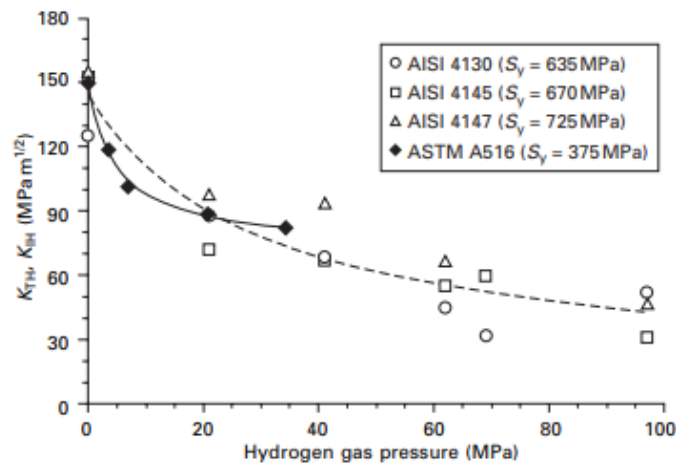


Fig. 11. Effect of gas pressure on fracture toughness in hydrogen gas(K_{IH}) or the threshold stress-intensity factor for propagation of cracks in hydrogen gas(K_{TH}) [34].

4.5 Effect of temperature

The permeability and diffusivity tests were done at 40°C. . Hydrogen gas is transported in pipelines typically at ambient temperatures. Hydrogen embrittlement is one of the most critical issues for hydrogen transfer pipelines operating at temperatures below 50°C [40]. For every structural metal, the effect of temperature on permeability and diffusivity does not follow a common trend. As temperature rises, low-alloy and carbon ferritic steels show less severe hydrogen embrittlement [34]. This trend is illustrated in Fig. 12, which shows that for AISI 4130 low-alloy steel, the threshold stress intensity factor (K_{TH}) for fracture propagation in hydrogen gas increases as temperature rises. The steel's solid solution of hydrogen causes hydrogen embrittlement, as shown in Fig. 12, across the entire temperature range. At temperatures higher than 473 K, hydrogen attack in carbon steels is one of the other

hydrogen embrittlement mechanisms that can be triggered in steels.

Most austenitic stainless steels have a maximum hydrogen embrittlement sensitivity at a temperature close to 200K and like ferritic alloys, become less susceptible at higher temperatures. Fig. 13 illustrates the former behaviour, which demonstrates that several austenitic stainless steels exhibit their lowest relative ductility between 200 K and 250 K [34]. A relative ductility value of 1 indicates the absence of hydrogen embrittlement. In metastable austenitic stainless steels, low temperatures have the effect of encouraging strain-induced martensite, which allows hydrogen embrittlement. Although austenitic stainless steels typically exhibit a maximum in hydrogen embrittlement at relatively low temperatures, this is not always the case; at least one alloy exhibits a minimum close to room temperature [35, 36].

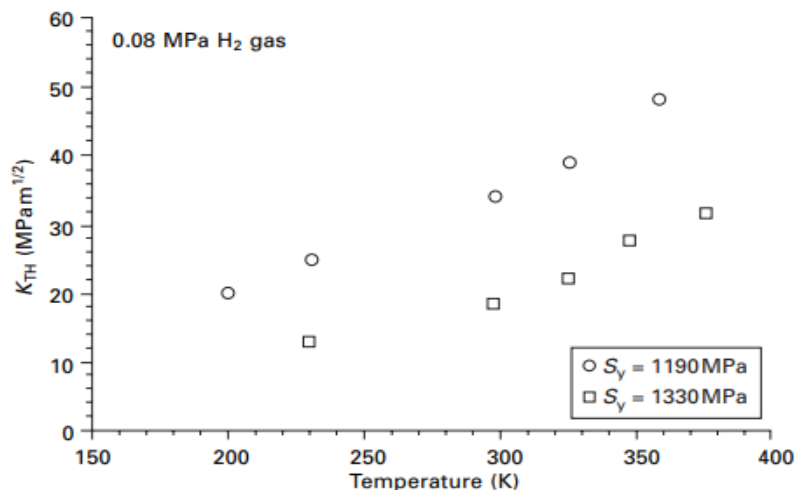


Fig.12. Effect of temperature on the threshold stress intensity factor (K_{TH}) for the propagation of cracks in hydrogen gas 4130 low-alloy ferritic steel [34].

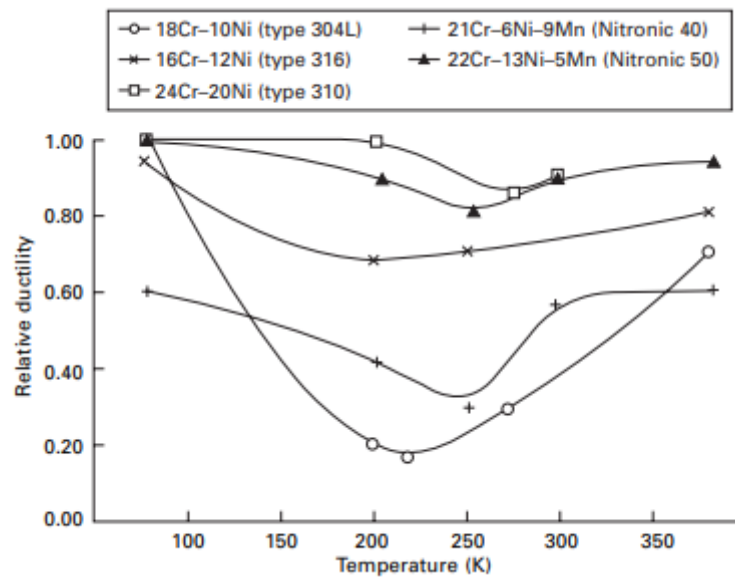


Fig. 13. Temperature effect on the ratio of tensile fracture strain in hydrogen-exposed and non-exposed test pieces for various austenitic stainless steels [34].

4.5 Effect of hydrogen barring coating

As expressed in Equation 3, barrier technology can reduce the hydrogen concentration gradient in the direction of test piece permeation. In general, the hydrogen barring coating may function as a physical barrier, lowering the

concentration of hydrogen in the pipe substrate and the flow of hydrogen permeation. The hydrogen concentration distribution along the test pieces' thickness direction is shown in Fig. 14.

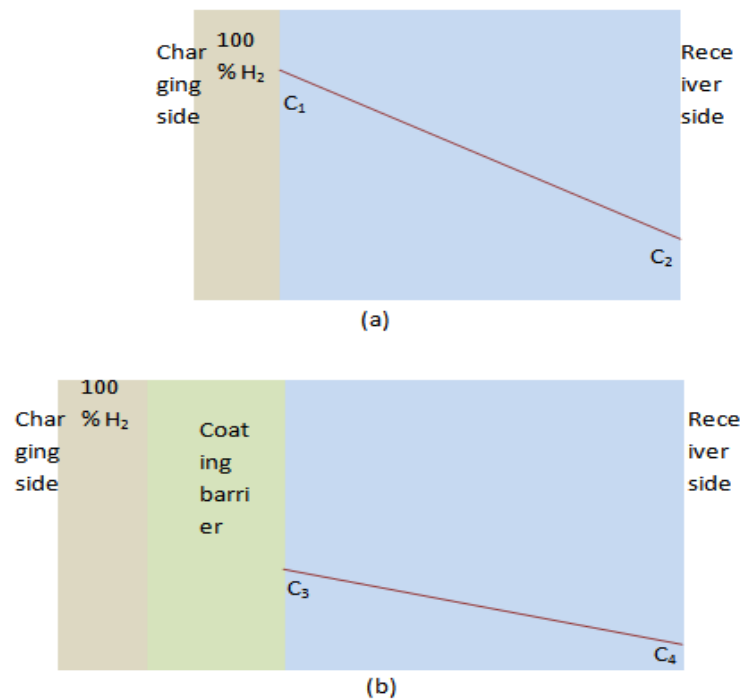


Fig. 14. Hydrogen concentration distribution (a) without a coating barrier (b) with a coating barrier.



Hydrogen management uses barrier technology to reduce concentration gradients. The flux of hydrogen through the walls of steel pipelines depends on concentration gradients and diffusivity. The reduction in concentration gradient would consequently lead to a reduction in permeability. Fowler et al. [39] originally suggested that a hydrogen barrier coating applied to the surface of stainless steel could delay or stop the migration of hydrogen atoms in the metal. The three primary attributes of an effective barrier are the capacity to inhibit or prevent hydrogen adsorption, a high permeation reduction factor, and the lack of structural flaws such as cracks and pores.

V. CONCLUSION

The impact of hydrogen pressure on hydrogen diffusivity and permeability was examined in this work. A high-pressure hydrogen testing instrument was used to conduct the test on three grades of pipe produced under different conditions.

The results of this study indicate higher permeability and diffusivity for pipes with heterogeneous microstructures. The results also depict an increase in hydrogen permeability and diffusivity with higher hydrogen pressure. It is recommended to select low-strength steel pipes (PSL-2, API 5L X52, or lower-grade pipes) and steel pipes with higher microstructure homogeneity for hydrogen transportation [17]. The purpose of low-strength steel pipes is to ensure that the weld and base metal hardness are within an acceptable range to minimize the occurrence of hydrogen embrittlement [17].

Acknowledgments

The author would like to thank Dr. Fabian Okoh and Engr. Nobert Oshoke for their support in proofreading this article.

VI. REFERENCES

- [1]. Pacific Northwest National Laboratory (2023). Hydrogen Compared with Other Fuels. Hydrogen Tools [Internet]. [Cited 2023 Aug 4]. Available from: <https://h2tools.org/hydrogen-compared-other-fuels>.
- [2]. National Grid (2023). What is Hydrogen? National Grid [Internet]. [Cited 2024 Jan 2]. Available from: <https://www.nationalgrid.com/national-grid-ventures/hydrogen>.
- [3]. European Industrial Gases Association (2023). IGC Doc 121/04/E: Hydrogen Transportation Pipelines [cited 2023 Aug 10]. Available from: <https://www.scribd.com/document/72194739/Hydrogen-Transportation-Pipelines>.
- [4]. Hydrogen and Fuel Cell Technologies Office (2023). Hydrogen Pipelines. Office of Energy Efficiency & Renewable Energy [internet]. [Cited 2023 Aug 6]. Available from: <https://www.energy.gov/eere/fuelcells/hydrogen-pipelines>
- [5]. Suresh, S. et al. (2005). Hydrogen Permeability and Integrity of Hydrogen Transfer Pipelines. Oak Ridge: Oak Ridge National Laboratory.
- [6]. Xu, K. (2012). Hydrogen Embrittlement of Carbon Steels and their Welds. Gaseous Hydrogen Embrittlement of Materials in Energy Technologies, 526-561. <https://doi.org/10.1533/9780857093899.3.526>.
- [7]. Osabohien H., Orumwense F., Ebulilo P., and Sadjere G. (2021). Investigation of Alternating Current Density and its Effect on Corrosion of Underground Hydrocarbon Pipelines. Nigerian Research Journal of Engineering Environmental Sciences, ID RJEES-06-93, 6(2) 2021 pp. 561-573 p ISSN: 2635-3342; ISSN: 2635-3350; 2021. <http://doi.org/10.5281/zenodo.5805161>.
- [8]. Suzuki, A., & Yukawa, H. (2020). A Review for Consistent Analysis of Hydrogen Permeability through Dense Metallic Membranes. Membranes, 10(6), 120. <https://doi.org/10.3390/membranes10060120>.
- [9]. Feng, Z. et al. (2007). Permeation, Diffusion, Solubility Measurements: Results and Issues. Oak Ridge: Oak Ridge National Laboratory, US Department of Energy.
- [10]. Lee, J. (2016). Hydrogen Embrittlement. National Aeronautics and Space Administration Marshall Space Flight Center Alabama, USA: NASA/TM-2016-218602.
- [11]. Kappes, M. A., & Perez, T. E. (2023). Blending Hydrogen in Existing Natural Gas Pipelines: Integrity Consequences from a Fitness for Service Perspective. Journal of Pipeline Science and Engineering, 3(4), 100141. <https://doi.org/10.1016/j.jpse.2023.100141>.
- [12]. TWI (2024). What is Hydrogen Embrittlement? Causes, Effects, and Prevention. TWI Ltd [internet]; [Cited 2024 Jan 22]. Available from: <https://www.twi-global.com/technical-knowledge/faqs/what-is-hydrogen-embrittlement>
- [13]. ASTM G1459-06 (R2012). Standard Test Method for Determination of Susceptibility of Metallic Materials to Hydrogen Gas Embrittlement (HGE). Philadelphia.
- [14]. Kumar, S. (2014). Hydrogen Embrittlement: Causes, Effects, and Prevention. Department of Metallurgical and Materials Engineering, NIT – Rourkela, 769008.
- [15]. Devanathan, M. and Stachurski, Z. (1962). Proceedings of Royal Society. A270, 90-102.
- [16]. API 5L (2004). Specification for Line Pipe. American Petroleum Institute, 49 CFR 192.113. Washington D.C.



- [17]. EIGA (2004). Hydrogen Transportation Pipelines. IGC Doc 121/04/E. European Industrial Gases Association, Brussels.
- [18]. Yokogawa (2022). Hydrogen Permeation. Oprex Field Instruments, Yokogawa Electric Corporation, Tokyo.
- [19]. Laadel, N., El Mansori, M., Kang, N., Marlin, S., & Boussant-Roux, Y. (2022). Permeation Barriers for Hydrogen Embrittlement Prevention in Metals – A Review on Mechanisms, Materials Suitability and Efficiency. *International Journal of Hydrogen Energy*, 47(76), 32707-32731. <https://doi.org/10.1016/j.ijhydene.2022.07.164>.
- [20]. Mohtadi-Bonab, M., & Masoumi, M. (2023). Different Aspects of Hydrogen Diffusion Behavior in Pipeline Steel. *Journal of Materials Research and Technology*, 24, 4762-4783. <https://doi.org/10.1016/j.jmrt.2023.04.026>.
- [21]. Cottis, R. (2010). Hydrogen Embrittlement. *Shreir's Corrosion*, 902-922. <https://doi.org/10.1016/B978-044452787-5.00200-6>.
- [22]. Popov, B. N., Lee, J., & Djukic, M. B. (2018). Hydrogen Permeation and Hydrogen-Induced Cracking. *Handbook of Environmental Degradation of Materials (Third Edition)*, 133-162. <https://doi.org/10.1016/B978-0-323-52472-8.00007-1>.
- [23]. Neelcon Steel (2024). API 5L X42 Pipe. Neelcon Steel Industries. [Internet]. [Cited 2024 Mar 3]. Available from: <https://www.neelconsteel.com/api-5l-gr-x42-carbon-steel-pipes.html>.
- [24]. Permanent Steel Manufacturing (2017). Chemical Composition of Carbon Steel Pipes. [Internet]. [Cited 2024 Mar 2]. Available from: <https://www.permanentsteel.com/newshow/chemical-composition-of-carbon-steel-pipes.html>.
- [25]. American Piping Product (2024). API 5L Seamless & Welded Pipe. [Internet]. [Cited 2024 Mar 4]. Available from: <https://amerpipe.com/products/api-5l-pipe-specifications/>.
- [26]. Park, D., & Liang, J. (2023). Effects of Temperature on Fatigue Crack Growth Rates of Low-carbon Pipe Steel in the Ductile and Ductile-to-Brittle Transition Regions. *Journal of Pipeline Science and Engineering*, 3(4), 100139. <https://doi.org/10.1016/j.jpse.2023.100139>.
- [27]. Nagao, A. et al. (2016). Gas-Phase Hydrogen Permeation Test Device and Method of Protecting Gas-Phase Hydrogen Permeation Test Device. *WO/2016/147596 A1*.
- [28]. Kumar V. (2022). Experimental Investigation of Fracture Behavior and Microstructure of API 5LX60 Line Pipe. *Materials Today: Proceedings*, 56, 595-608. <https://doi.org/10.1016/j.matpr.2021.12.149>.
- [29]. Contreras, A., Quej-Aké, L., Lizárraga, C. et al. (2015). The Role of Calcareous Soils in SCC of X52 Pipeline Steel. *MRS Online Proceedings Library 1766*, 95-106. <https://doi.org/10.1557/opl.2015.416>.
- [30]. Scimed (2024). A Brief Introduction to SEM (scanning electron microscopy). [Internet]. [Cited 2024 Mar 3]. Available from: <https://www.scimed.co.uk/education/sem-scanning-electron-microscopy/>.
- [31]. Weyand, H. (2021). What is the Difference Between Austenitic, Ferritic, and Martensitic Stainless Steel. [Internet]. [Cited 2024 Mar 3]. Available from: https://www.aatprod.com/hrf_faq/what-is-the-difference-between-austenitic-ferritic-and-martensitic-stainless/.
- [32]. Souza, R. et al. (2017). Effect of Microstructure on Hydrogen Diffusion in Weld and API X52 Pipeline Steel Base Metals under Cathodic Protection. *International Journal of Corrosion*, Vol. 2017, Article ID 4927210. <https://doi.org/10.1155/2017/4927210>.
- [33]. Jian, X., & Xiukui, S. (1993). Hydrogen Permeation and Diffusion in Low-Carbon Steel and 16Mn Steel. State Key Laboratory of RSA, Institute of Metal Research, Academia Sinica, Shenyang, 110015, China
- [34]. Somerday, B., & San Marchi, C. (2008). *Solid-State Hydrogen Storage*. 3: 51-81. Woodhead Publishing, ISSN 978-1-84569-270-4.
- [35]. Holbrook, J. & AJ West, A. (1981). The Effect of Temperature and Strain Rate on the Tensile Properties of Hydrogen Charged 304L, 21-6-9, and JBK 75', in *Hydrogen Effects in Metals*, IM Bernstein and AW Thompson, Eds., The Metallurgical Society of AIME, New York, pp. 655-63.
- [36]. Ma, L., Liang, G., & Li, Y. (1992). Effect of Hydrogen Charging on Ambient and Cryogenic Mechanical Properties of a Precipitate-Strengthened Austenitic Steel', in *Advances in Cryogenic Engineering*, Vol. 38A, FR Fickett and RP Reed, Eds., Plenum Press, New York, pp. 77-84.
- [37]. Caskey, G. (1983). *Hydrogen Compatibility Handbook for Stainless Steels (DP-1643)*, EI du Pont Nemours, Savannah River Laboratory, Aiken, SC.
- [38]. Li, Q., Ghadiani, H., Jalilvand, V., Alam, T., Farhat, Z., & Islam, M. (2024). Hydrogen Impact: A Review on Diffusibility, Embrittlement



- Mechanisms, and Characterization. *Materials*, 17(4). <https://doi.org/10.3390/ma17040965>.
- [39]. Fowler, J. et al. (1977). Tritium Diffusion in Al_2O_3 and BeO . *J. Am. Ceram. Soc.*, 60(3-4), 155-161.
- [40]. Mohitpour, M., Pierce, C., & Hooper, R. (1988). The design and engineering of cross-country hydrogen pipelines. Novacorp International Consulting Inc. Calgary.